

**jmr&t**

Journal of Materials Research and Technology

www.jmrt.com.br



## ORIGINAL ARTICLE

# Ultra Grain Refinement During the Simulated Thermomechanical-processing of Low Carbon Steel

Alberto Moreira Jorge Junior<sup>1,\*</sup>, Luiz Henrique Guedes<sup>1</sup>, Oscar Balancin<sup>1</sup><sup>1</sup>Department of Materials Engineering, Universidade Federal de São Carlos, São Carlos, Brazil.

Manuscript received February 25, 2012; in revised form September 6, 2012.

Grain refinement is a useful method to improve the strength and toughness of steels without changing their chemical composition. In this study, critical temperatures for the thermomechanical treatment of niobium microalloyed steel were determined experimentally and through thermodynamic data. Simulations of conventional and controlled thermomechanical processing and a thermomechanical treatment to obtain ultrafine-grained microstructures were conducted using torsion tests. The final microstructures displayed significant grain size refinement. Conventional processing produced grains with an average size of 12  $\mu\text{m}$ , while controlled processing led to an average grain size of 4.9  $\mu\text{m}$  and severe plastic deformation at warm temperatures resulted in a grain size of 1.3  $\mu\text{m}$ . The ultra refinement of ferrite grains was associated with strain-induced dynamic phase transformation and dynamic recrystallization of as-transformed ferrite.

**KEY WORDS:** Grain refinement; Ultrafine grain; Physical simulation.

© 2012 Brazilian Metallurgical, Materials and Mining Association. Published by Elsevier Editora Ltda.

Este é um artigo Open Access sob a licença de [CC BY-NC-ND](#)

## 1. Introduction

It is well-known that low-carbon low-alloy steels today are the grades yielding the highest production volumes at the lowest cost. These materials have a wide range of applications, albeit limited to low strain loads. One method to increase mechanical strength and toughness is microstructure refinement. Reduction of the average grain size can be achieved in several ways upon processing. During thermal treatments, control of phase transformation parameters such as temperature, holding time, and cooling rate reduces the average grain size. In hot rolling or hot forging, control of the recrystallization kinetics during arrest

times between deformations leads to significant grain size refinement<sup>[1,2]</sup>. In microalloyed steels, grain refinement is achieved by controlling the precipitation/recrystallization interaction during hot rolling<sup>[3-6]</sup>. The final microstructure of these grades is attained during thermomechanical processing, with no additional heat treatments.

Recent researches involving metallic materials can lead to technological innovations<sup>[7]</sup>. Both advanced thermomechanical processes and severe plastic deformation strategies have been developed to obtain ultrafine ferrite grain with size close to 1  $\mu\text{m}$  in low-carbon low-alloy steels<sup>[8]</sup>. Advanced thermomechanical processes involving modification to conventional large-scale processes can be optimized to operate in deformation conditions where they beneficially exploit solid-solid reactions such as recrystallization, precipitation, and phase transformation.

\*Corresponding author.

E-mail address: moreira@ufscar.br (A. M. Jorge Junior)

Ultrafine grain size has been obtained in steels through deformation near or in the intercritical region by exploiting strain-induced dynamic transformation<sup>[9-11]</sup>. Ferrite dynamic recrystallization can be exploited straining in warm condition inside the ferrite domain<sup>[12,13]</sup>. Also, ultrafine or nanocrystalline structures has been achieved by warm or cold deformation of martensite starting microstructure<sup>[14-16]</sup>.

The strength of low-carbon low-alloy steels would undoubtedly increase significantly and their range of applications expanded if ultrafine microstructures were achieved. However, to find the processing route for refining the microstructure, the phenomena that take place must be known and the appropriate schedule to control these phenomena during processing must be determined. This kind of development can be done by standard production equipments but, usually, it is not economically practicable. Another way is through laboratory simulation, replying the processing parameters. The purpose of this work was to simulate the grain refinement routes currently in use and to investigate a new thermomechanical treatment attempting to obtain an ultrafine-grained microstructure close to 1  $\mu\text{m}$  for low-carbon low-alloy steel. In this treatment, unstable austenite was subject to a severe deformation.

## 2. Critical Temperatures

During thermomechanical treatments, ingots, plates, and blocks are heated up to austenitization temperatures and soaked at these temperatures for some time, then strained on a multipass schedule under continuous cooling conditions, and cooled to room temperature. Fig. 1 is a schematic representation of the thermomechanical treatment for microalloyed steel, indicating the critical temperatures ( $T_s$ ,  $T_{nr}$ ,  $A_{R3}$ , and  $A_{R1}$ ). Upon heating, austenite nucleates at the  $\text{Fe}_3\text{C}/\alpha$  interface and grows, completely consuming the ferrite and cementite which is present at room temperature<sup>[17,18]</sup>. Inside the austenite domain, as the temperature rises, the compounds present as precipitates dissolve until the whole material becomes austenitic. For niobium microalloyed steels, the Nb-carbonitride solubi-

lization temperature ( $T_s$ ) can be calculated using Irvine's solubility product equation [Eq. 91)]<sup>[19]</sup>:

$$\log \left[ \%Nb \cdot \left( \%C + \frac{12}{14} \%N \right) \right] = 2,26 - \frac{6770}{T_s}$$

The dissolution of the precipitates is completed by heating to temperatures above the  $T_s$  and grain growth takes place during soaking. Thus, the deformation schedule begins with a completely austenitic material and a coarse-grained microstructure. The imposed deformation schedule changes the shape of the ingots, plates or slabs and continually alters the material's microstructure. Two types of procedures are used to deform austenite: conventional or controlled thermomechanical processing<sup>[5]</sup>. The former consists of multi-deformation schedules aimed at changing the shape, while the second also aims to control the microstructural evolution.

Controlled thermomechanical processing has been successfully industrialized in modern steel mills and can be defined as disciplined deformation schedules under continuous cooling and controlled conditions, aimed at attaining fine-grained microstructures<sup>[3-6]</sup>. This kind of processing can be separated in four different stages, as the temperature decreases. In the first stage, grains coarsened by soaking at temperatures above  $T_s$  are refined by the repetition of deformations and recrystallizations at high temperatures. The second stage takes place under conditions in which recrystallization is no longer completed during interpass times due to strain-induced precipitation<sup>[20,21]</sup>, i.e., below the non recrystallization temperature ( $T_{nr}$ ). Grains in this stage have a pancake-like shape and dislocation substructures are created inside the grains.

In the third stage, deformation takes place in the phase transition region, i.e., in the temperature range between the start of ferrite formation ( $A_{R3}$ ) and the end of ferrite transformation ( $A_{R1}$ ). Ferrite nucleates within and at grain boundaries. In this stage, austenite continues to deform and the transformed ferrite begins to be strained. In the fourth stage, a variety of microstructures can be obtained during cooling, depending on the cooling rate and the stage in which the deformation was interrupted. After the first deformation stage, when the material is air-cooled, the ferrite grains are relatively large due to grain growth during cooling. After the second stage, the grains are smaller. In the third stage, increasing the cooling rate causes the grains to become finer and substructural dislocation occurs inside the strained ferrite grains.

During conventional thermomechanical processing, the multi-deformation schedule is similar to that of the first stage, where the recrystallization kinetics is very fast. Thus, static recrystallization occurs during interpass times and no strain accumulates from one pass to another.

It is well-established that the start temperature of ferrite formation ( $A_{R3}$ ) and the end temperature of this transformation ( $A_{R1}$ ) depend on the cooling rate. These temperatures decrease as the cooling rate is increased. When higher cooling rates are imposed, austenite is present at temperatures below that of equilibrium between the phases ( $A_{E3}$  and  $A_{E1}$ ). Thus, it is possible to deform unstable austenite<sup>[8-10]</sup>. Upon deformation, strain-induced dynamic phase transfor-

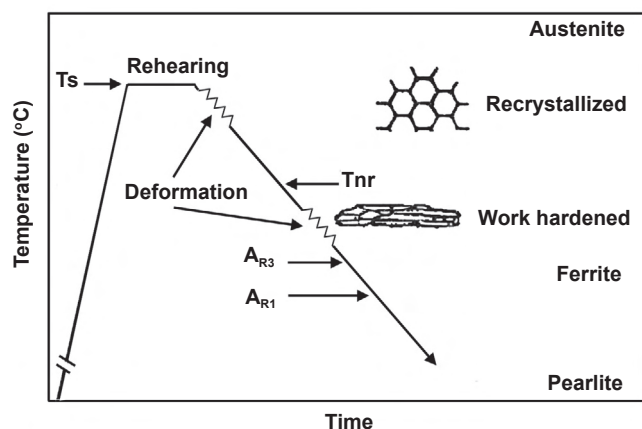


Fig. 1 Schematic representation of the thermomechanical treatment for microalloyed steel, indicating the critical temperatures

mation (austenite to ferrite) can take place. New ferrite grains and transformed ferrite during cooling are strained together with austenite and continuous dynamic recrystallization of ferrite can occur.

### 3. Material and Procedures

The material used in this work was supplied by Villares Metals S.A., Sumaré, SP, Brazil. The measured chemical composition is described in Table 1, which indicates that this low carbon steel is microalloyed with niobium. The as received bars with a diameter of 35 mm were reheated to 1,200°C, held at this temperature for 30 min, and hot-rolled to a thickness of 15 mm. The samples used in this work were machined from the hot-rolled bars.

To determine some of the critical temperatures, dilatometry tests were carried out using 2 mm diameter, 12 mm long samples. These samples were heated to 1,150°C at a rate of 2°C/s, held at this temperature for 10 min and continually cooled at rates varying from 1°C/s to 9°C/s.

Thermomechanical treatments were simulated on a computerized hot torsion machine. Cylindrical specimens with 5 mm of effective radius and 10 mm of effective length in the reduced central gage were reheated in an infrared radiation furnace coupled directly in the test machine. Chromel-alumel thermocouples were used to measure the test temperatures. To prevent oxidation, the samples were protected by a quartz tube through which argon was injected. The data were collected using a software program that imposed test parameters such as temperature, interpass time, amount of strain, strain rate, and heating and cooling rates.

Two kinds of hot torsion tests were performed: multiple passes under continuous cooling conditions and a single deformation after continuous cooling. Deformations under continuous cooling conditions were conducted to determine the critical temperatures and to simulate conventional and controlled thermomechanical processing and single severe deformation after continuous cooling was conducted to obtain an ultrafine microstructure.

In all experiments with multiple passes under continuous cooling, samples were heated to 1,200°C at a rate of 1.7°C/s. After 600 s at this temperature, the samples were continuously cooled at a rate of 1°C/s and subjected to schedules of deformations. In these multipass schedules, identical strain of 0.3 was applied, at an identical strain rate of 1 s<sup>-1</sup>, followed by identical interpass times of 30 s. After the tests, the samples were air-cooled to room temperature. Fig. 2a schematically represents the applied thermomechanical cycle. To determine the critical temperatures, 20 passes were applied during cooling. The initial and final deformation temperatures were 1,200°C and 630°C. To simulate conventional thermomechanical processing, the samples were subjected to 7 passes. The initial and final deformation temperatures were 1,200°C and 1,020°C.

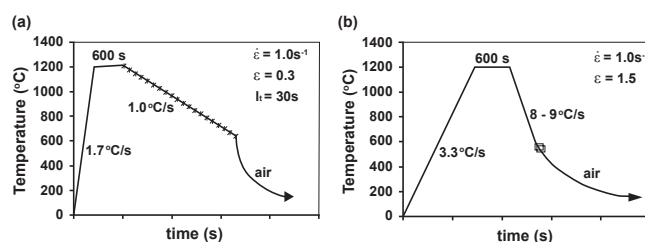


Fig. 2 (a) Schematic representation of the multipass tests under continuous cooling conditions; (b) schematic representation of the thermomechanical treatment to obtain an ultrafine microstructure

To study controlled processing the samples were subjected to 12 deformations between 1,200°C and 870°C.

In the experiments aimed at obtaining an ultrafine microstructure, the imposed heating rate was 3.3°C/s. The samples were heated to 1,200°C and held at this temperature for 600 s. In these simulations, instead of straining under continuous cooling conditions, a single deformation was imposed (Fig. 2b). The samples were cooled at a rate of 8°C/s to 9°C/s to temperatures below  $A_{E1}$  and strained to 1.5 using a strain rate of 1 s<sup>-1</sup>, followed by air-cooling. Three experiments were carried out with an identical thermomechanical cycle, changing only the deformation temperatures: 625°C, 575°C, and 545°C.

The resulting physical simulated microstructures were observed through optical and scanning electron microscopy. The average grain sizes were determined with the aid of the image analysis software analySIS Pro 3.1. The misorientation between grains/subgrains was determined using an Electron Backscattered Diffraction Equipment (EBSD) from TexSEM Laboratories (TSL), model MSC-2200, coupled to a Philips XL30-FEG (Field Emission Gun) high-resolution scanning electron microscope.

The specimens for microstructure observations were collected in the torsion sample surface in a perpendicular plane to the transverse direction and prepared according to the classical procedure (mechanical grinding and polishing up to a 1 µm diamond paste) followed by 2% nital etching. Samples for EBSD were prepared by an additionally sub-micron polishing with silica colloidal for about 3 hours before the observations. The grain size was measured in at least 10 different fields of each sample by means of optical microscopy, by following the ASTM E112-96 standard, and by SEM in at least 50 different fields of each sample at a magnification of more than 10<sup>4</sup> and, in both cases, the results were averaged.

### 4. Results

The solubilization temperature calculated using Irvine's solubility product equation [Eq. (1)] was 1,150°C. The equilibrium temperatures between phases calculated using Thermo-Calc® software were  $A_{E1} = 879^\circ\text{C}$  and  $A_{E3} = 727^\circ\text{C}$ . The transformation temperatures under different cooling rates measured by dilatometric tests are presented in Table 2, together with the calculated temperatures and those determined by torsion tests.

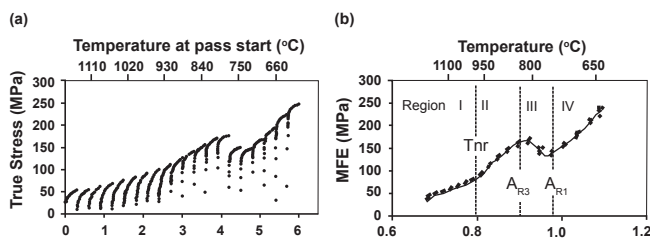
Fig. 3a displays data from multipass torsion tests under continuous cooling conditions conducted to determine processing critical temperatures. Fig. 3 indicates that the plas-

Table 1 Chemical composition of the steel under study (wt. %)

C	Si	Mn	S	P	Al	Nb	N
0.076	0.49	1.36	<0.005	<0.005	0.011	0.04	0.004

**Table 2** Measured and calculated critical temperatures. The numbers between parentheses indicate the cooling rates used in the test

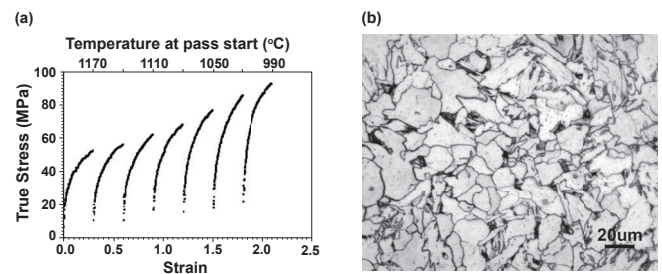
	Temperature (°C)					
	T <sub>s</sub>	T <sub>nr</sub>	A <sub>R3</sub>	A <sub>R1</sub>	A <sub>E3</sub>	A <sub>E1</sub>
Irvine equation	1,150					
Torsion test (1°C/s)		989	842	722		
(1°C/s)			804	682		
(3°C/s)			735	614		
Dilatometer (5°C/s)			717	575		
(7°C/s)			702	543		
(9°C/s)			687	526		
Thermo-Calc®					879	727

**Fig. 3** a) Typical flow curves for experiments conducted to determine the thermomechanical treatment critical temperatures: T<sub>nr</sub>, A<sub>R3</sub> and A<sub>R1</sub>; and (b) evolution of mean flow stress (MFS) as a function of the inverse of deformation temperatures determined from five experiments

tic flow stress level changes with the deformation schedule and hence, with the deformation temperature; at higher temperatures the stress increases as deformation temperatures decline, and this increment increases as the temperature declines. After reaching a maximum, the stress decreases, but begins to rise again at lower temperatures. Fig. 3b clearly reveals the stress level variations. In this diagram, the mean flow stress (MFS) is plotted as a function of the inverse of deformation temperature determined from five experiments. The changes in the curve's slopes indicate the critical temperatures<sup>[22]</sup>.

The changes in the stress levels are associated with the microstructure evolution that occurs during the multi-deformation schedule<sup>[3-6]</sup>. The initial microstructure consists of larger austenite grains. Upon testing in region I, the material is work-hardened during deformation and the deformed grains recrystallize in the interpass times. At the end of each interpass time, the microstructure consists of equiaxial grains. In region II, the static recrystallization does not complete in the interpass times and strain accumulation from one pass to the next takes place. In the region III, the gamma/alpha transformation occurs and new equiaxial ferrite grains are present and begin to be strained. These new grains are work-hardened in region IV and recrystallize and grow upon cooling after deformation.

Fig. 4 displays data from torsion tests simulating conventional multi-deformation schedule. In these experiments, the initial and final deformation temperatures were 1,200°C and 1,020°C. It can be seen in Fig. 4a that in each

**Fig. 4** (a) Typical flow curves for experiments conducted to simulate conventional thermomechanical processing; and (b) final microstructure depicting ferrite grains with an average size of 12 μm

pass the stress increases with deformation; after the arrest time the shape of the next flow curve is similar to the previous one, but the stress level is something higher than that of the former deformation. One can infer the material was softened during interpass times and the increment in the mean flow stress is due to the temperature decrease. Comparing the procedures used in this simulation with the non recrystallization temperature (T<sub>nr</sub>) measured, it can be seen that all the deformations occurred in region I of Fig. 3b, indicating that static recrystallization was completed in each interpass time. Fig. 4b depicts the microstructure observed after deformation and indicates recrystallized grain with an average size of 12 μm measured in three experiments.

In the experiments conducted to simulate the controlled thermomechanical processing, the samples were subjected to a 12-deformation-schedule between 1,200°C and 870°C. Fig. 5a shows the flow stress curves attained in one of these experiments. It can be seen in Fig. 5a that the amount of softening in the interpass times change; after the first deformation there is full softening while in the last passes there are strain accumulations: the level of stress increases continuously in the last passes. As a consequence, upon phase transformation the number of nucleation sites raised since the material was work-hardened. In this procedure, deformation took place in regions I and II of the Fig. 3b. Fig. 5b shows the microstructure observed after the simulation, indicating grain refinement; the average grain size determined in three experiments was 4.9 μm.



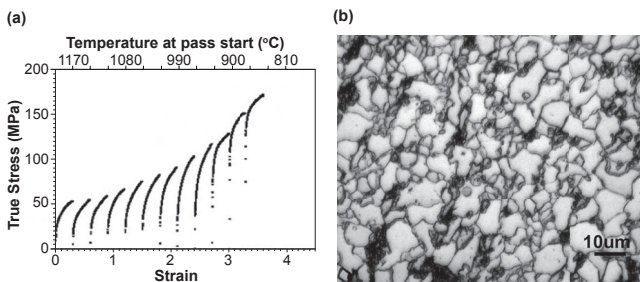


Fig. 5 (a) Typical flow curves for experiments conducted to simulate controlled thermomechanical processing; and (b) final microstructure depicting ferrite grains with an average size of 4.9  $\mu\text{m}$

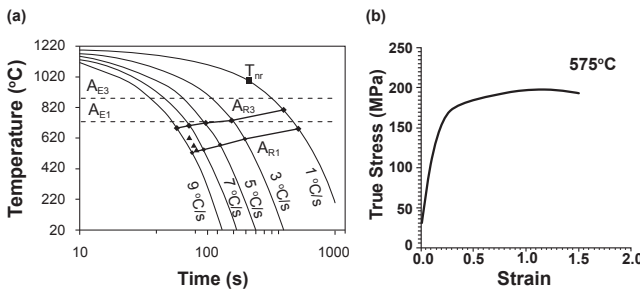


Fig. 6 (a) CCT diagram indicating the equilibrium temperatures between phases and the temperatures in which deformations were applied to obtain ultrafine microstructures; and (b) typical flow stress curve measured during straining after cooling

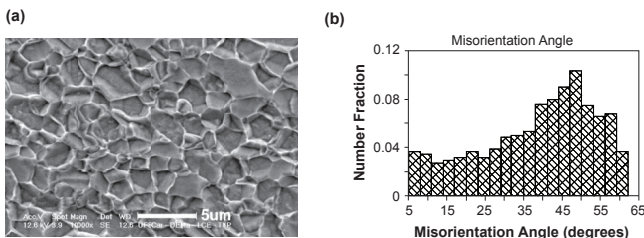


Fig. 7 Photomicrograph of a sample deformed in the intercritical region (625 °C), presenting ferrite grains with an average size of 1.5  $\mu\text{m}$ ; and (b) distribution of grain/subgrain misorientation size measured by EBSD

In the experiments aimed at obtaining ultrafine microstructures, a single severe deformation was imposed after continuous cooling. The applied deformation was carried out after cooling with a rate of 8 °C/s to 9 °C/s, as highlighted in the continuous cooling transformation diagram (CCT) depicted in Fig. 6a. Also, it is showed in this diagram the values of the equilibrium temperatures between phases. It is possible to see that unstable austenite was deformed in all experiments; the starting temperatures were between  $A_{R1}$  and  $A_{R3}$ , however below  $A_{E1}$ . The flow stress curve is depicted in Fig. 6b. Comparing the stress level observed in Fig. 6a with that presented in Fig. 3a, it is worth noting that at same temperature the level of stress is lower in unstable austenite.

Fig. 7a shows a SEM photomicrograph of the microstructure and Fig. 7b displays the EBSD misorientation angle distribution diagram. Bearing in mind that misorientations smaller than 15 degrees indicate subgrains and larger than 15 degrees grains and, as can be seen in (Fig. 6b), close to 30% of the boundaries are subgrain boundaries and 70% are grain boundaries, one can infer that the material was recrystallized.

The average grain size obtained at the aforementioned deformation temperatures were 1.5  $\mu\text{m}$ , 1.3  $\mu\text{m}$ , and 1.3  $\mu\text{m}$ .

## 5. Discussion

Comparing the reheating temperature applied in the simulations conducted here against the value calculated through Irvine's equation (Table 2), it can be inferred that, in each simulation, the niobium carbonitrides were totally dissolved after the soaking time. In the conventional thermomechanical processing simulations, seven consecutive deformations were applied with the last pass at 1,020 °C. A comparison of this temperature with the  $T_{nr}$  measurement (Table 2) indicates that all deformations occurred in the first stage of the thermomechanical processing, i.e., complete recrystallization took place between passes. Conventional processing usually produces ferrite grains with sizes of around 20  $\mu\text{m}$  to 30  $\mu\text{m}$ , and the minimum average size attained was close to 10  $\mu\text{m}$ <sup>[23]</sup>. Particularly in the simulation carried out here, the grains obtained had an average size of 12  $\mu\text{m}$ . This value is close to the lowest limit and may be attributed to the solute drag effect promoted by niobium in solution, inhibiting the grain growth<sup>[5]</sup>.

In controlled thermomechanical processing simulations, the final deformation was applied at 870 °C, which is a temperature lower than  $T_{nr}$ . Thus, deformations also occurred in the second stage, i.e., complete recrystallization did not occur between passes and strain was retained from one pass to the next. In this kind of processing, grain refinement is promoted in first passes by repeated austenite recrystallization, like in conventional processing. At temperature below  $T_{nr}$ , retained strain increase the number of nucleation sites for gamma/alpha transformation. In these simulations, ferrite grains with an average size of 4.9  $\mu\text{m}$  were obtained. The minimum average grain size that has been obtained in industrial processing is limited to around 4  $\mu\text{m}$  to 5  $\mu\text{m}$ . This limit, which seems to exist in industrial processing, does not depend on the amount of deformation imposed on austenite. Instead, it is probably determined by ferrite grain growth during cooling<sup>[24,25]</sup>.

The thermomechanical treatments applied here to obtain ultrafine-grained microstructures responded by producing grains with an average size close to 1  $\mu\text{m}$ . Fig. 6b shows that the final microstructure is composed of 70% of grains and 30% of subgrains, characterizing a recrystallized material. An analysis of the procedures and results obtained from these experiments indicates that microstructural refinement is associated with large deformations in intercritical domains (between  $A_{R3}$  and  $A_{R1}$ ) under accelerated cooling. At the beginning of deformation, the microstructure is composed of austenite and ferrite. When the ferrite is being deformed, it hardens, recovers and recrystallizes, generating new grains. Also, as austenite is deformed, taking into account that austenite is a low stacking fault energy material; a typical dislocation substructure is formed inside the remaining austenitic grains. The dislocation cell walls are regions of high free energy and become sites for ferrite nucleation, bringing about strain-induced transformation of the unstable austenite.

Analogously to the microstructure evolution observed by the authors in the ferrite to austenite strain-induced dynamic transformation<sup>[18]</sup>, it is suggested that the gamma/



Fig. 8 Schematic representation of the austenite to ferrite strain-induced dynamic transformation mechanism<sup>[18]</sup>

alpha transformation occurs with the ferrite nucleation inside the remaining austenite grains, as schematically shown in Fig. 8. Thus, the application of large deformations under accelerated cooling condition tends to: (i) enhance diffusion  $\gamma \rightarrow \alpha$  transformation; and (ii) activate dynamic phenomena such as dynamic recrystallization and strain-induced dynamic phase transformation, which bring about continual deformation on an already refined microstructure.

All data displayed in this work were attained by physical simulation in laboratory scale, or by mathematic calculations. Physical simulation tries to reply industrial processing. However, the geometry of processing was not respected in this work; all attention was paid in processing parameters such as temperature, strain, strain rate and interpass times. By one hand, with this procedure it is easier to conduct one investigation on the role of processing parameters and to analyze the attained data. For instance, the simulation of conventional and controlled processing makes clear in which conditions the material softening by static recrystallization or strain is retained from one pass to the next due to precipitation/recrystallization interaction.

By other side, in a new procedure, the required technologies to conduct the industrial processing are not evaluated. For instance, in the treatments applied here to obtain ultrafine-grained microstructures, it was imposed cooling rate of around 9°C/s. Applying such as rate in industrial hot rolling mills will not be easy; certainly will be a temperature gradient between surface and middle of the strip or plate, becoming the microstructure evolution different from that described here. However, upon forging of small components, these levels of cooling rate and applied strain can be imposed and an ultrafine-grained microstructure will be attained, rising the mechanical strength of low-carbon low-alloy steels.

## 6. Conclusions

- The physical simulations conducted here engendered information about the phenomena that occurred during multi-deformation schedules: work-hardening, softening, phase transformations and microstructure evolution;
- simulation of established industrial processes such as conventional and controlled processing makes possible to investigate the role of processing parameters; as deformation temperature was decreased in multi-deformation schedule, softening by static recrystallization was not completed in interpass times;
- the physical simulations conducted here in the laboratory scale indicated that it is possible to attain ultrafine-grained microstructures in low-carbon steels. Grain size of

microalloyed steel that is usually refined to 5  $\mu\text{m}$  in controlled rolled mills can be reduced to around of 1  $\mu\text{m}$  by severe deformation of unstable austenite.

## References

1. Sellars CM. Computer modeling of hot-working process. *Mater Sci Technol* 1985; 1:325-31.
2. Maccagno TM, Jonas JJ, Hodgson PD. Spreadsheet modeling of grain size evolution during rod rolling. *ISIJ International* 1996; 36:720-8.
3. Tanaka T. Controlled rolling of steel plate and strip. *Int Metals Rev* 1981; 4:185-212.
4. Jonas JJ, Sellars CM. Thermomechanical processing. In: Charles JA, Greenwood GW, Smith GS (eds.). *Future development of metals and ceramics*. Cambridge: Woodhead Publishing Limited; 1992.
5. DeArdo AJ. Modern thermomechanical processing of microalloyed steel: A physical metallurgy perspective. *Proc. Microalloying'95 Conf.*, June 11-14, 1995. Pittsburgh, PA: The Iron and Steel Society, 1995; p. 15-33.
6. Jonas JJ. In: Yue S (ed.). *Microstructural evolution during hot rolling. Proceedings of the International Symposium on Mathematical Modeling of Hot Rolling of Steel*; 1990 August 26-29; Hamilton (Ont) Canada. Warrendale (PA): Iron and Steel Soc. of AIME, 1990; 99-118.
7. Howe AA. Industry perspective on ultrafine grained steels. *Mater Sci Technol* 2009; 24:815-9.
8. Song R, Ponge D, Raabe D, Speer JG, Matlock DK. Overview of processing, microstructure and mechanical properties of ultrafine grained bcc steels. *Mater Sci Eng A* 2006; 441(1):1-17.
9. Niikura N, Fujioka M, Adachi A, Matsukura A, Yokota T, Shirota Y, et al. New concepts for ultra refinement of grain size in Super Metal Project. *JMPT* 2001; 117:141-6.
10. Beladi H, Kelly GL, Shokouhi A, Hodgson PD. The evolution of ultrafine ferrite formation through dynamic strain-induced transformation. *Mater Sci Eng A* 2004; 371(1-2):343-52.
11. Abdollah-Zadeh A, Eehbali B. Mechanism of ferrite grain refinement during warm deformation of a low carbon Nb-microalloyed steel. *Mater Sci Eng A* 2007; 457(1-2):219-25.
12. Najafi-Zadeh A, Jonas JJ, Yue S. Grain refinement by dynamic recrystallization during the simulated warm-rolling of interstitial free steels. *Metallurgical Transactions A* 1992; 23A: 2607-16.
13. Narayana Murthy SVS, Torizuka S, Nagai K. Ferrite grain size formed by large strain-high Z deformation in a 0.15C steel. *Materials Transactions* 2005; 46:2454-60.
14. Ueji R, Tsuji N, Minamino Y, Koizumi Y. Ultragrain refinement of plain low carbon steel by cold-rolling and annealing of martensite. *Acta Mater* 2002; 50:4177-89.
15. Tsuji N, Maki T. Enhanced structural refinement by combining phase transformation and plastic deformation in steels. *Scripta Mater* 2009; 60:1044-9.
16. Hase K, Tsuji N. Effect of initial microstructure on ultrafine grain formation through warm deformation in medium-carbon steels. *Scripta Mater* 2011; 65:404-7.
17. Speich GR, Demarest VA, Miller RL. Formation of austenite during intercritical annealing of dual-phase steels. *Mettal Trans A* 1981; 12:1419-28.
18. Oliveira MAF, Jorge Jr. AM, Balancin O. Influence of strain-induced nucleation on the kinetics of phase transformation in a forging steel during warm working. *Scripta Mater* 2004; 50:1157-62.
19. Irvine KJ, Pickering FB, Gladman T. Grain-Refined C-Mn Steels. *Journal of The Iron and Steel Institute* 1967; 205:161-80.
20. Dutta B, Palmiere EJ, Sellars CM. Modelling the kinetics of strain induced precipitation in Nb microalloyed steels. *Acta Mater* 2001; 49(5):785-94.

21. Dutta B, Palmiere EJ. Effect of prestrain and deformation temperature on the recrystallization behavior of steels microalloyed with niobium. *Metall Mater Trans A* 2003; 34:1237-47.
22. Borato FJ, Barbosa R, Yue S, Jonas JJ. Effect of chemical composition on the critical temperature of microalloyed steels. *Proc Int Conf on Physical Metallurgy of Thermomechanical Processing of Steels and Other Metals (Thermec-88)*, June 1988. Tokyo, Japan: ISIJ, 1988; p.383-90.
23. Priestner R, Al-Horr YM, Ibraheem AK. Effect of strain on formation of ultrafine ferrite in surface of hot rolled microalloyed steel. *Mater Sci Technol* 2002; 18:973-80.
24. Priestner R, Hodgson PD. Ferrite grain coarsening during transformation of thermomechanically processed C-Mn-Nb austenite. *Mater Sci Technol* 1992; 8:849-54.
25. Novillo E, Cotrina E, Iza-Mendia A, López B, Gutiérrez I. Factors limiting the achievable ferrite grain refinement in hot worked microalloyed steels. *Mater Sci Forum* 2005; 500-501:355-62.